Oxidation at Defects in Scales on Iron-Chromium Alloys

J.H. Swisher, W.D. Cho, and W.W. Qiu

A prior investigation on the lateral spreading of oxide into defects in Wustite scales on iron was extended to study the same phenomena in Fe-Cr alloys. Included were two Fe-Cr-Mo alloys and an Fe-25Cr-6Al alloy. Three types of experiments were conducted to study flaws introduced to simulate damage to protective oxide layers caused by particle erosion. It was found that outer scales of Wustite on the Cr-Mo alloys spread into flaws in much the same way as Wustite on unalloyed iron. However, inner scales of $(Fe,Cr)_3O_4$ on the Cr-Mo alloys and the scale formed on the Fe-25Cr-6Al alloy had only a slight tendency to spread into flaws. These results are consistent with the known higher diffusion coefficients and higher defect concentrations in Wustite than in other oxide phases.

1 Introduction

BECAUSE iron-chromium alloys have good resistance to thermal oxidation, their properties are discussed extensively in the literature on metal oxidation and hot gas corrosion.[1-4] For the research to be described here, a relevant series of articles was published in a symposium book on corrosion of steels in CO_2.[5-7] Depending on alloy composition and exposure conditions, the oxide phases formed may be Cr_2O_3, Fe-Cr spinels, iron oxides with dissolved chromium, and duplex scales containing two or more phases. Kofstad[8] and others have studied the oxidation of pure iron in CO-CO_2 gas mixtures, but the results have little applicability to Fe-Cr alloys.

Secondary oxidation at cracks and flaws in oxide scales has not been studied extensively. Schutz[9] investigated the formation and healing of flaws in high-chromium alloy steels during thermal cycling. He found there to be a critical strain rate below which healing occurred by the formation of a new oxide in the cracks. In 1989, a symposium was held on the combined effects of corrosion and erosion.[10] An article in this book by Swisher, Cho, and Chang[11] examined oxidation at defects in FeO scales on unalloyed iron. This research was a precursor to the work described here. It was found that lateral diffusion in FeO scales occurred sufficiently fast to contribute to the smoothing of scratches or grooves made in the scale. These defects were designed to simulate damage to the oxide caused by abrasive particles. The results discussed in Ref 11 are extended in the present study to examine the same effects in Fe-Cr alloys.

J.H. Swisher and **W.W. Qiu,** Department of Mechanical Engineering and Energy Processes, Southern Illinois University at Carbondale, Carbondale, Illinois. **W.D. Cho,** Department of Metallurgical Engineering, University of Utah, Salt Lake City, Utah.

2 Experimental Conditions

The compositions of the alloys used as specimen materials are listed in Table 1. Alloys in the Fe-Cr-Mo series are commonly used in boiler tubes and oil refinery plants and are commercially available. Specimens of these alloys were procured

Fig. 1 Scanning electron micrograph of 9Cr-1Mo specimen after preoxidation for 13 hr at 900 °C with $CO/CO_2 = 1.76$.

Table 1 Experimental Alloy Compositions

Alloy designation	Composition, wt% Cr	Mo	Ni	Al	Other elements
7Cr-½Mo steel	6.9	0.6	0.3	...	0.1 C, 0.4 Mn, 0.6 Si
9Cr-1Mo steel	8.3	1.0	0.1	...	0.1 C, 0.5 Mn, 0.6 Si, 0.1 Cu
Fe-25Cr-6Al	24.6	...	<0.01	5.9	0.004 C, <0.01 Mn, <0.01 Si

from Metal Samples Co., Inc., Munford, Alabama. The Fe-25Cr-6Al alloy was obtained from a large quantity of material prepared by the Carpenter Steel Co. for evaluation in research projects on structural materials for high-temperature coal processing applications.

An attempt was made to preoxidize specimens for experiments on secondary oxidation at defects by duplicating the procedure of a prior investigator.[6] Unfortunately, the scales formed under these conditions were either very thin or were nonadherent. It was found that temperatures in the range from 900 to 1150 °C were needed for preoxidation to produce acceptable oxide scales for experiments with defects. These treatments were carried out in a Lindberg controlled atmosphere tube furnace in CO-CO_2 gas mixtures and in air. H_2-H_2O gas mixtures, which were used in the precursor study on pure iron,[11] were not considered appropriate because they could cause hydrogen attack and/or extensive surface decarburization.

Figure 1 shows a scanning electron micrograph (SEM) of a 9Cr-1Mo specimen after a preoxidation treatment at 900 °C. The top layer of FeO partially spalled from the surface, showing an adherent layer of $(Fe, Cr)_3O_4$ spinel over the metal surface. Identification of these oxide phases was made by X-ray diffraction. A few cracks can be seen in the spinel layer. These cracks were not present when specimens were preoxidized at 1150 °C.

Three types of experiments were conducted to study oxidation at defects. In one type, preoxidized specimens containing scribed defects were reheated in evacuated and sealed Vycor capsules. In a second type, similar specimens were re-exposed to the same gas atmosphere as used for preoxidation. In both types of experiments, defects were normally cut through the scales with a wire saw. The wire used was 0.25 mm diam and contained diamond dust in a steel matrix. On occasions when the scale was less than 10 micrometers in thickness, a diamond scriber was used instead of the wire saw. In the third type of experiment, platinum bands were diffusion bonded into grooves in the alloy to simulate bare metal at the base of a flaw. The lateral growth of oxide over the platinum bands was then studied by heating the specimens in an oxidizing atmosphere. These procedures will be discussed further in the "Results and Discussion" section.

The specimens were characterized using X-ray diffraction, optical microscopy, scanning electron microscopy (SEM), energy dispersive X-ray analysis (EDX), and Auger electron spectroscopy (AES).

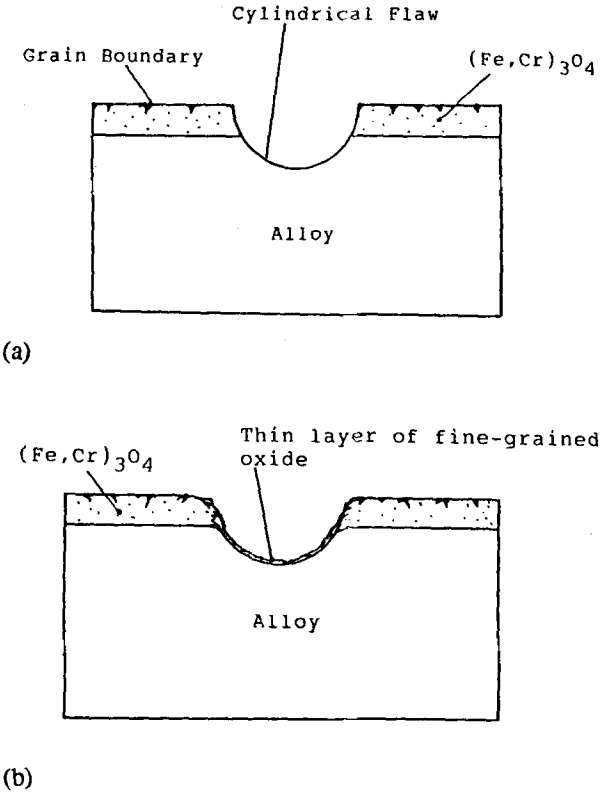

Fig. 2 (**a**) Cylindrical flaw made with wire saw in preoxidized Cr-Mo steel specimens. (**b**) Spreading of oxide into flaw during thermal anneal in static vacuum.

3 Results and Discussion

Oxidation-resistant alloy steels have invariably been developed around the idea that one or more alloying elements facilitate the formation of adherent oxide scales. Because of their adherence and low diffusion coefficients of oxygen and alloying elements, metal loss due to oxidation is slow. If the concentrations of these alloying elements are sufficiently high, damage to the oxide scale should be self-healing, because the desired oxide phases can continue to form. However, if there is extensive dam-

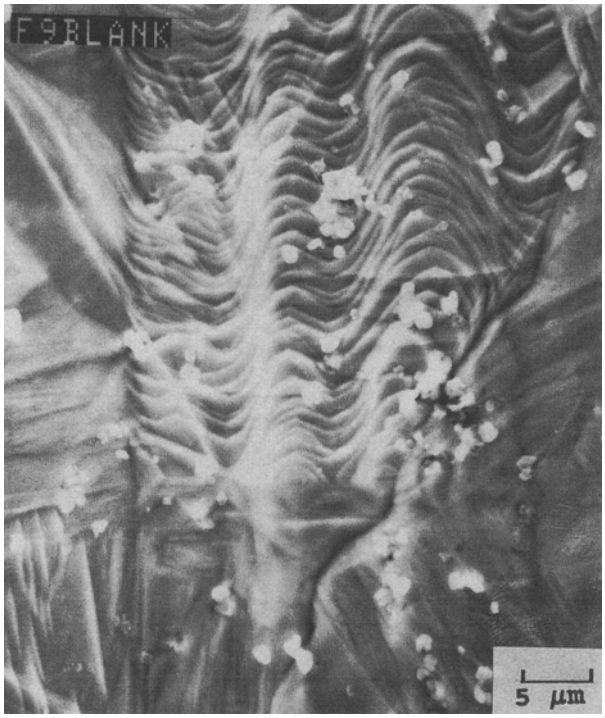

Fig. 3 Unoxidized 9Cr-1Mo specimen with flaw after annealing in evacuated capsule for 3 days at 900 °C.

Table 2 Oxide Composition in Flaws Healed in Static Vacuum

Alloy designation	Preoxidation conditions: Temperature, °C	Time, hr	Atmosphere	Healing conditions: Temperature, °C	Time, hr	Oxide composition: Outside flaw	Inside flaw
7Cr-½Mo steel	1150	16	$CO/CO_2 = 1.76$	900	160	Cr/Fe = 0.66	Cr/Fe = 0.27
9Cr-1Mo steel	1150	16	$CO/CO_2 = 1.76$	900	160	Cr/Fe = 1.02	Cr/Fe = 0.57
Fe-25Cr-6Al	1150	16	$CO/CO_2 = 1.76$	900	160	Cr/Fe = 0.53	Cr/Fe = 0.77
						Al/Fe = 3.63	Al/Fe = 1.03
Fe-25Cr-6Al	1150	48	Air	900	116	Cr/Fe = 2.00	Cr/Fe = 0.87
						Al/Fe = 13.83	Al/Fe = 1.35

age to protective scales from eroding particles, metal loss due to oxidation can be extensive, particularly if the concentration of alloying elements is low.

There is a possibility that lateral spreading of protective oxide layers over defects caused by eroding particles could lessen their harmful effects. It is this possibility that was the focus of the research described here. For a description of the mechanism by which striations and scratches on a solid surface can disappear at high temperature, the interested reader is referred to a classic paper by Chalmers, King, and Shuttleworth.[12] These authors showed that, with surface free energy or capillarity as the driving force, striations on a silver surface formed or disappeared, depending on the gas atmosphere. They were able to make an artificial groove on a silver surface disappear in 20 min at 850 °C. Surface diffusion was believed to be the most important mass transport mechanism. There has been an extensive amount of work since Ref 12 was published on metal specimens and unpublished work by S. Barbezat and J. Philibert[13] covered healing of scratches on aluminum oxide.

Although the behavior may be more complex, capillarity effects could contribute to the manner in which oxide forms in defects in scales. In Ref 11, it was shown that FeO scales on iron will spread laterally into or over grooves made in the scales. Calculations showed that a vaporization-condensation mechanism involving iron atoms did not apply, but surface or bulk diffusion could account for the observations. In the extension of this work to Fe-Cr alloys, the results of three types of experiments will be discussed in sequence.

3.1 *Sealed Capsule Experiments*

The first step in these experiments was to preoxidize specimens at 1150 °C for a sufficient length of time to obtain a spinel layer at least several micrometers in thickness. The FeO outer layer that had not spalled off was easily removed mechanically. Flaws were made on the surface, as depicted in Fig. 2(a). The specimens were then sealed in evacuated Vycor capsules. As shown in Fig. 2(b), reheating caused lateral spreading of oxide into the flaws to occur. The thickness, composition, and structure of the oxide formed in the flaws were the parameters studied.

It is appropriate to discuss the steps taken to ensure that little or no direct oxidation of the specimens occurred during these experiments. It was important to heat all of the capsule surfaces before sealing to pump out condensed and adsorbed moisture. The weights of the specimens were measured before and after each experiment to check for instances when the necessary precautions were not taken. Figure 3 shows the results of another test of the sealing procedure. An unoxidized 9Cr-1Mo alloy specimen was annealed in a sealed capsule for 3 days at 900 °C. The SEM micrograph was taken at a location where a scribed flaw was made on the surface. The white particles could be the result of slight oxidation or of contamination during metallographic preparation, probably the latter. In general, the surface was bright and shiny, which contrasts with the other specimens to be discussed, where the spreading of oxide produced a pronounced darkening of their surfaces.

The experimental conditions and oxide compositions for four sealed capsule experiments are listed in Table 2. Low concentrations of Mo, Si, and Mn were also detected in the oxides, but not listed in the table. The data were obtained by EDX, and a relatively large sampling area was used to average effects of impurities and inhomogeneities. The first two entries show data for the 7 and 9% Cr alloys. The important result for these specimens is that the Cr content of the oxide formed in the flaws was only about half that in the oxide adjacent to the flaws. It is possible that this effect is due to slower lateral diffusion of Cr into the flaws. Hodge[14] measured diffusion coefficients of Cr and Fe in spinel using radioactive tracers. The diffusion coefficients varied with oxygen partial pressure, but D_{Cr} was always 10^3 times lower than D_{Fe} at 1200 °C. Because the ionic radii of Cr and Fe are nearly equal, the difference in diffusivities cannot be explained by a size effect. The explanation given by Hodge was that Cr exists as Cr^{3+}, whereas Fe is present predominately as Fe^{2+}. The difference leads to coulombic interactions, which result in a lower jump frequency for Cr^{3+}.

It is useful to compare D_{Fe} in the spinel with D_{Fe} in FeO. From the data of Himmel *et al.*[15] for FeO, the comparison shows that Fe diffuses 150 or more times slower in the spinel than in FeO at 1200 °C. This difference contributes to the ability of the spinel to provide oxidation protection, but it also tends to make the lateral spreading of spinel-type oxide into flaws rather slow.

Although the Cr enrichment effect is consistent with rationale presented above on bulk diffusion rates, the effect could perhaps also be explained by relative surface diffusion rates or vaporization-condensation rates. No insight can be offered on the former, but preferential vapor transport of Fe compounds is a possibility. As shown by Surman and Castle,[16] the formation of $Fe(CO)_5$ vapor in CO atmospheres and $Fe(OH)_2$ vapor in steam atmospheres can affect the oxidation rates of iron and mild steel. Another potential contributor to lateral spreading of oxide is plastic flow. This mechanism is not believed to be important here because it is inconsistent with the Cr enrichment effect.

Scanning electron micrographs of the 7Cr-½Mo specimen are shown in Fig. 4. The structure of the oxide at the base of the

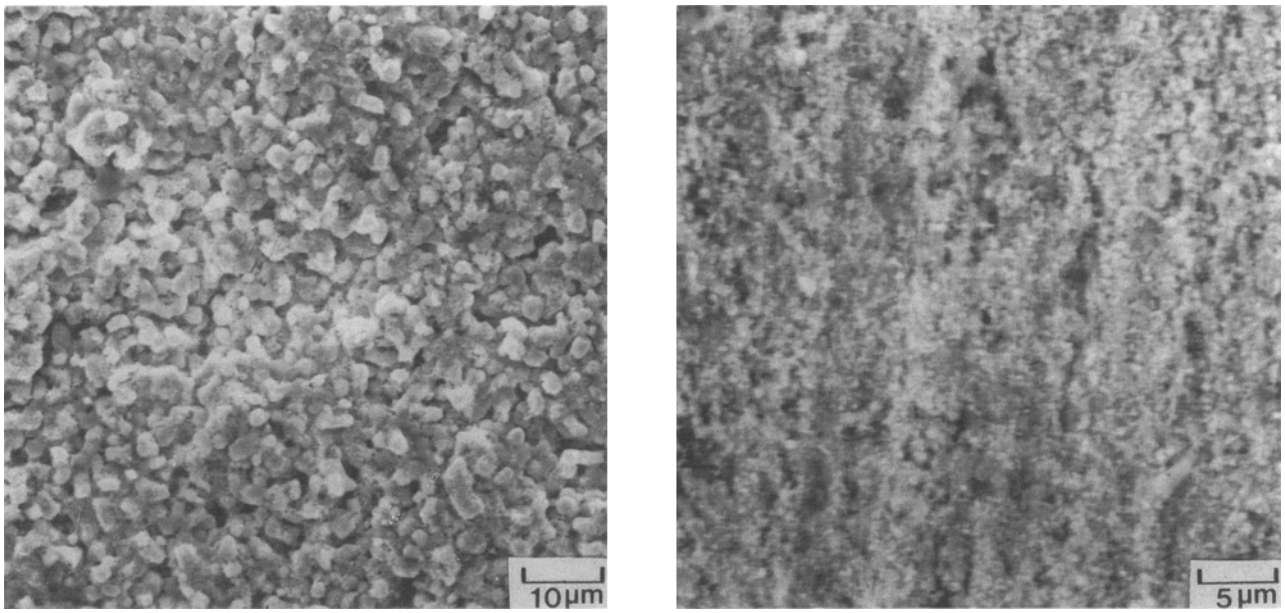

(a) (b)

Fig. 4 Scanning electron micrographs of 7Cr-0.5Mo alloy after reheating at 900 °C in static vacuum. (**a**) Outside flaw. (**b**) Inside flaw.

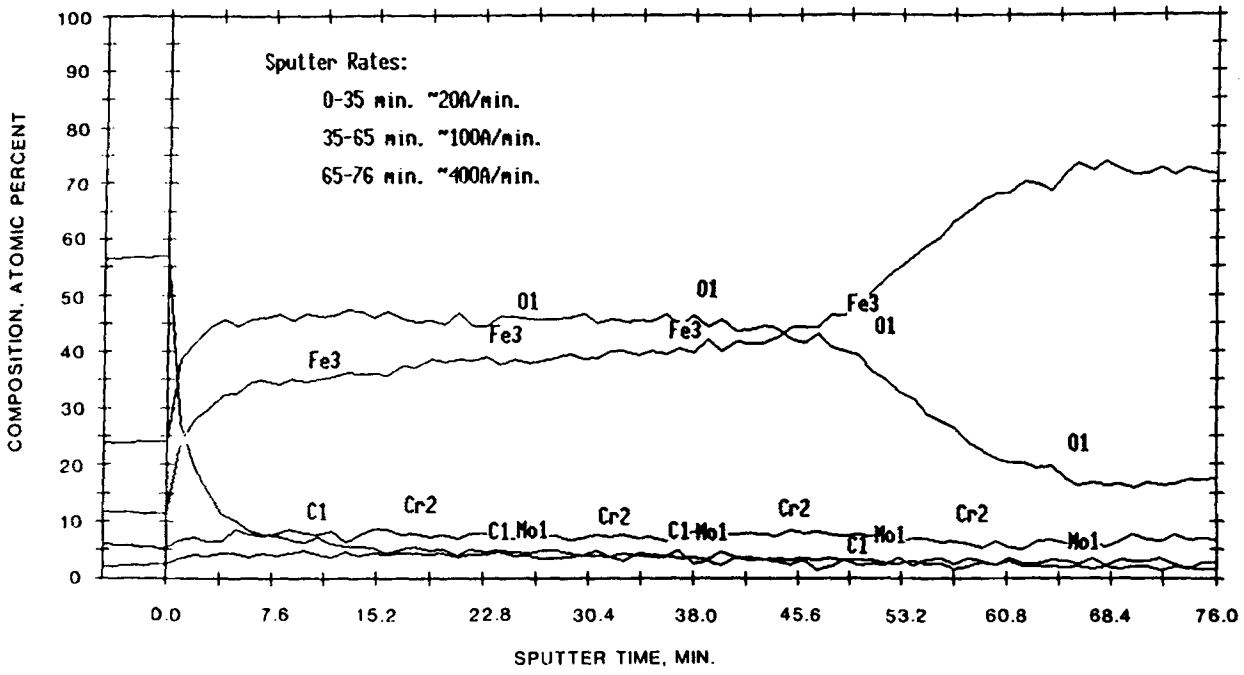

Fig. 5 Auger depth profile data for oxide at base of flaw in 7Cr-0.5Mo steel specimen shown in Fig. 4.

flaw shown in Fig. 4(b) is finer than for the oxide outside the flaw shown in Fig. 4(a). Within the flaw, individual grains of oxide are not resolvable, but some of the surface roughness from the wire saw is still evident in the oxide.

The same 7Cr-½Mo specimen was characterized by Auger electron spectroscopy (AES). The results of depth profile measurements in the flaw area are shown in Fig. 5. The Cr concentration appears to be between 5 and 10 at.% and changes only slightly with distance from the surface. However, analysis for Cr in steels by AES is not very accurate because of overlapping Cr and O spectra. In examining the Fe and O concentrations for sputtering times up to 47 min, it appears that the oxide is nonstoichiometric, with the Fe-O ratio increasing with depth. From the sputter rate, the oxide layer in the flaw is approximately 2000 Å (0.2 microns) thick. For longer sputtering times, it is likely that the beam is penetrating into the metal phase and is touching

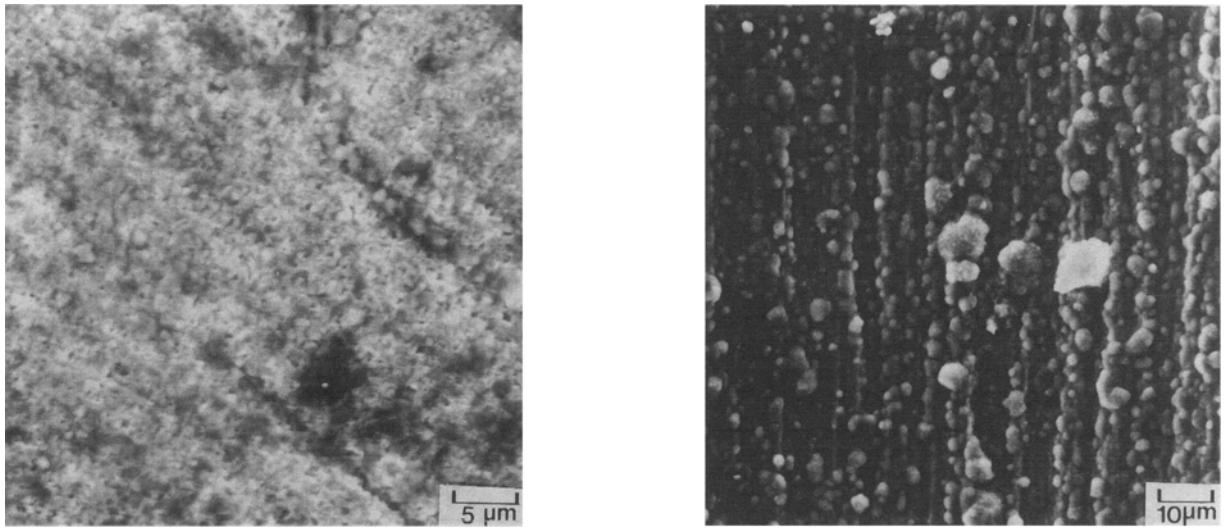

(a) (b)

Fig. 6 Scanning electron micrographs of Fe-25Cr-6Al alloy after reheating at 900 °C in static vacuum. (**a**) Outside flaw. (**b**) Inside flaw.

some oxide particles formed by internal oxidation. The AES results are generally consistent with the EDX results listed in Table 2, because both show a low Cr concentration in the oxide formed in the flaw.

The last two entries in Table 2 give results for Fe-25Cr-6Al specimens preoxidized and reheated under different conditions. In both cases, there was a significant depletion of aluminum oxide in the flaw area. This result parallels the results for Cr-Mo steels, in that slow lateral diffusion of one of the species, Al ions in this case, was probably responsible for the depletion effect. Because of the Al depletion, there is a corresponding enrichment of chromium oxide inside the flaws, which could give a protective character to the oxide layer formed there.

Figure 6 shows SEM micrographs of the Fe-25Cr-6Al specimen that had been preoxidized in the CO-CO_2 gas mixture, then heat treated in a capsule. The structure within the flaw in Fig. 6(b) is believed to consist of a thin layer of oxide covering the metal surface and discrete particles of oxide growing on top. This duplex structure was also observed with pure iron.[11] The structure adjacent to the flaw in Fig. 6(a) is unusual in that no oxide grains can be resolved.

3.2 *Reheating in Oxidizing Atmosphere*

In this series of experiments, the specimens were preoxidized and flaws made in the same manner as described above. Then the specimens were reheated in the same controlled atmosphere as was used for preoxidation. Experiments of this type simulate more closely service conditions for the material, but there is a drawback in that it is difficult to distinguish between lateral spreading of oxide into the flaw and new oxide formed by direct reaction with gaseous species.

The first experiment of this type was conducted on unalloyed iron, and the results are shown in Fig. 7. Figure 7(a) shows a flaw made in the FeO scale, and Fig. 7(b) shows the same location after reheating for $4\frac{1}{2}$ hr at 1150 °C. The grains are smaller where the two sides of the flaw grew together, but no indentation of the surface remained. Lateral spreading of the oxide was, therefore, extensive. Because CO was present in the gas phase, vapor transport by iron carbonyl formation could have occurred, or lateral diffusion of Fe^{2+} ions in the FeO could also explain the result. The structure in Fig. 7(b) is not believed to be consistent with a viscous flow mechanism.

The results of an experiment on a 9Cr-1Mo alloy specimen are given in Fig. 8. It is an SEM cross section of a flaw after heating for 24 hr at 900 °C. The outer scale was found by EDX to be FeO; the inner scale should be $(Fe, Cr)_3O_4$ and a zone of internal oxidation is also evident. There was no clear evidence for spreading of oxide into the flaw, and the zone of internal oxidation progressed deeper into the specimen at the location of the flaw. Both of these observations lead to the conclusion that direct reaction with the oxidizing gas was the dominant effect. However, there was a distinct difference in appearance between the flaw area and the adjacent material when viewed from above. The SEM micrographs in Fig. 9 show this difference. The outer scale inside the flaw in Fig. 9(b) has a fine, ledge-like appearance, whereas the scale adjacent to the flaw in Fig. 9(a) is coarse grained. This difference could be due simply to the time required for coarse grains to form.

Additional experiments of this type were carried out on the Fe-25Cr-6Al alloy. The results were essentially the same as for the Cr-Mo alloys. There was no clear evidence that lateral spreading of oxide into the flaws occurred.

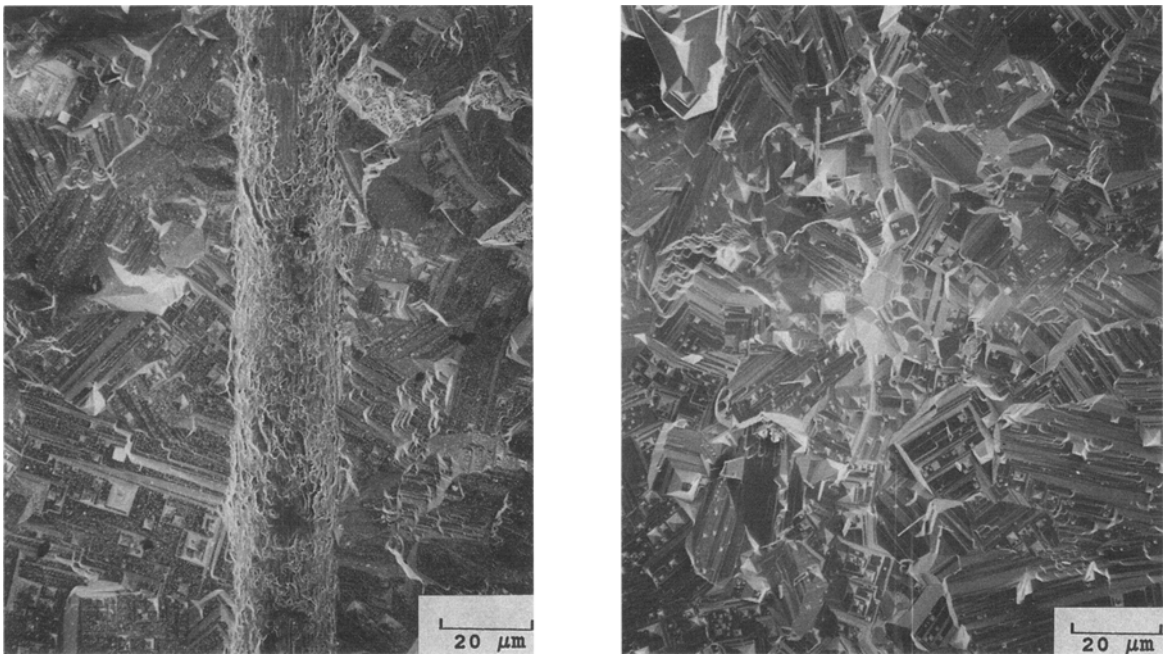

(a) (b)

Fig. 7 Reoxidation of unalloyed iron specimen. **(a)** Appearance of flaw made after preoxidation for 16 hr at 1150 °C with $CO/CO_2 = 1.76$. **(b)** Appearance of same flaw after heating for 4.5 hr at 1150 °C in same atmosphere.

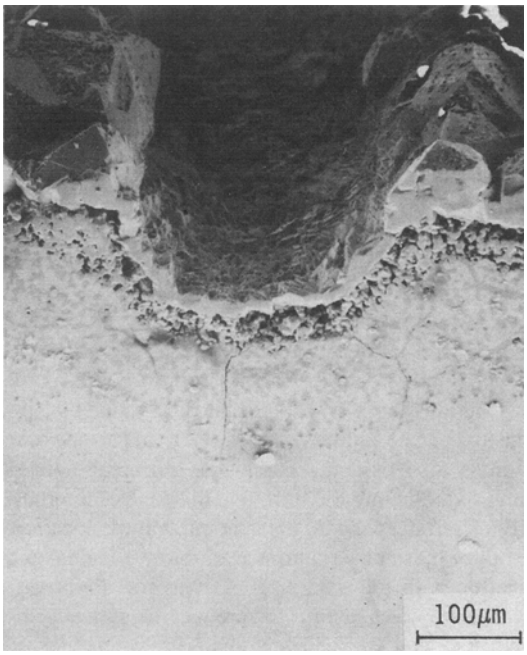

Fig. 8 Scanning electron micrograph of flaw in 9Cr-1Mo alloy after heating for 24 hr at 900 °C in gas mixture with $CO/CO_2 = 1.76$.

3.3 *Experiments with Noble Metal Simulated Defects*

The final set of experiments consisted of observing the extent to which an oxide scale will grow laterally over a platinum band embedded in the surface of a specimen. Specimens for these experiments were prepared by cutting grooves in the unoxidized surface with a wire saw. Then platinum wires were pressed into the grooves and diffusion bonded to the specimen by heat treating in a H_2 atmosphere at 1150 °C. Finally, the surface was polished to remove excess platinum.

The specimens were oxidized under various conditions to study the tendency of oxide formed on the alloy surface to extend over the Pt simulated defect. When this spreading occurs, metal-oxide and oxide-gas interfaces are created, and a metal-gas interface is eliminated. Because the free energy associated with the metal-gas interface is normally higher than the sum of the others, there is a thermodynamic driving force for the oxide to cover the exposed metal. The same argument applies to flaws cut through scales to expose bare metal, as was done in the capsule experiments.

The results of one of these experiments is shown in Fig. 10. The 9Cr-1Mo alloy was oxidized for 6 hr at 1150 °C in a gas mixture with $CO/CO_2 = 1.76$. Immediately after removal from the furnace, it was observed that a loosely adherent scale, presumed to be FeO, completely covered the Pt band. Figure 10 shows the appearance after removal of the loose scale. At first, it was thought that a spinel layer had also begun to grow over the Pt band, because the Pt band was narrower than before oxidation. However, Auger and EDX measurements on the portion of the sample adjacent to the exposed Pt proved that a Pt-Fe alloy or intermetallic layer had formed by diffusion.

Additional experiments of this type were carried out on the 9Cr-1Mo alloy at 900 °C and on the Fe-25Cr-6Al alloy at 1150 and 900 °C. In none of these experiments was there a significant amount of oxide growth over the platinum. In the prior study on unalloyed iron,[11] similar experiments were conducted with

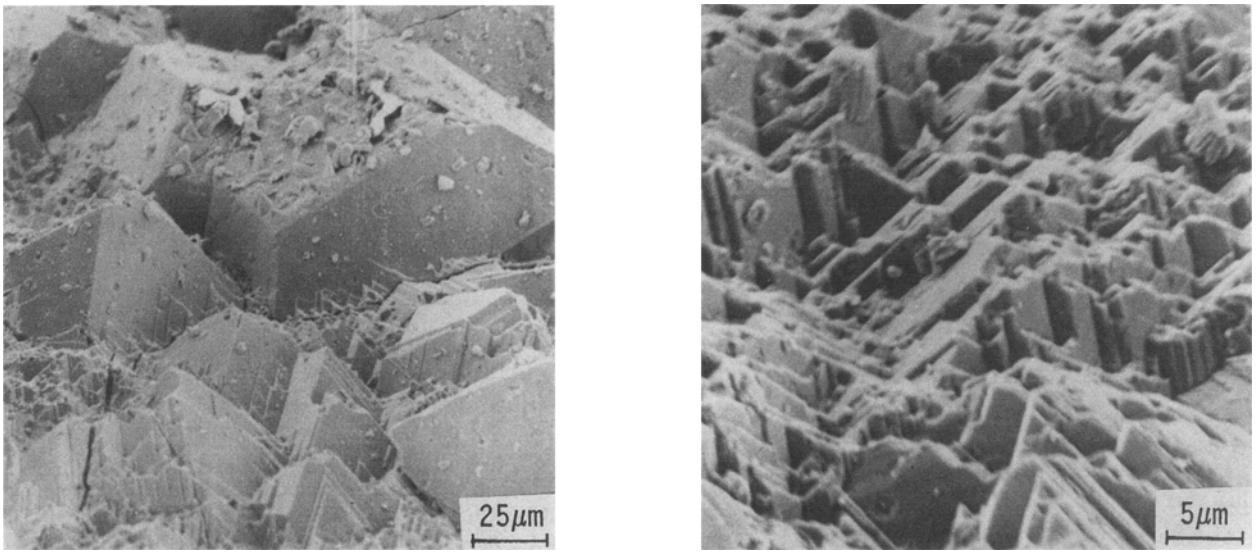

(a) (b)

Fig. 9 SEM top views of specimen from Fig. 8. (**a**) Outside flaw. (**b**) Inside flaw.

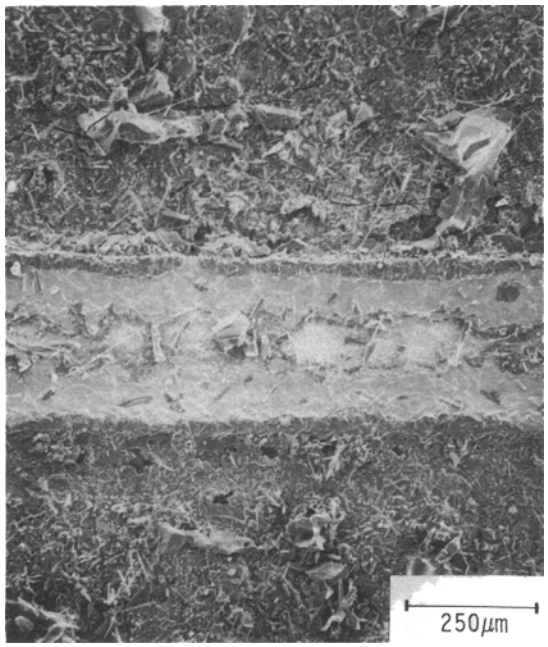

Fig. 10 Scanning electron micrograph showing surface of a 9Cr-1Mo alloy specimen containing a Pt band after oxidation at 1150 °C for 6 hr with $CO/CO_2 = 1.76$ and removal of nonadherent oxide.

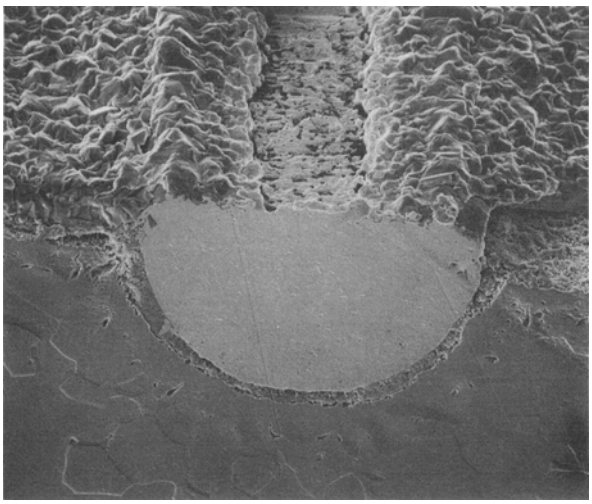

Fig. 11 Growth of FeO over gold band on unalloyed Fe at 720 °C.

gold rather than platinum bands. An example of the results obtained is reproduced in Fig. 11. It shows an FeO scale growing over a gold-simulated defect at 720 °C. Thus, FeO grows readily over flaws in both alloy steels and unalloyed iron, but other oxide phases with lower defect concentrations and diffusion coefficients do not.

4 Conclusion

When FeO formed as an outer scale on Cr-Mo steels, it had a tendency to spread into flaws in the scale in a similar fashion to FeO on unalloyed iron. Spinel compounds of the type $(Fe, Cr)_3O_4$ in inner scales showed much less tendency to spread into flaws, probably because of lower diffusion coefficients in the spinels compared to FeO. The scale formed on an Fe-25Cr-6Al

alloy also exhibited a low tendency toward spreading. The formation of volatile species of Fe, such as iron carbonyl, may have contributed to lateral mass transport into the flaws.

Acknowledgment

Financial support for this project was provided by the U.S. Department of Energy under Contract No. DE-FC22-89PC89904.

References

1. N. Birks and G.H. Meier, *Introduction to High Temperature Oxidation of Metals*, Edward Arnold Press, London (1983).
2. D.B. Meadowcroft and M.I. Manning, *Corrosion Resistant Materials for Coal Conversion Systems*, Elsevier Applied Science Publishers, New York (1984).
3. J.F. Norton, *High Temperature Materials Corrosion in Coal Gasification Atmospheres*, Elsevier Applied Science Publishers, New York (1984).
4. M.G. Rothman, *High Temperature Corrosion in Energy Systems*, Am. Inst. Mining, Metallurgical and Petroleum Engineers, New York (1985).
5. P.L. Harrison, R.B. Dooley, S.K. Lister, D.B. Meadowcroft, P.J. Nolan, R.E. Pendlebury, P.L. Surman, and M.R. Wootton, in *Proceedings of International Conference on Corrosion of Steels in CO_2*, D.R. Holmes, R.B. Hill, and L.M. Wyatt, Ed., British Nuclear Energy Society, 220-233 (1974).
6. M.G.C. Cox, B. McEnaney, and V.D. Scott, in *Proceedings of International Conference on Corrosion of Steels in CO_2*, D.R. Holmes, R.B. Hill, and L.M. Wyatt, Ed., British Nuclear Energy Society, 247-256 (1974).
7. P.L. Surman, J. Bettelheim, R.B. Dooley, J. Graham, D.B. Meadowcroft, and P.C. Rowlands, in *Proceedings of International Conference on Corrosion of Steels in CO_2*, D.R. Holmes, R.B. Hill, and L.M. Wyatt, Ed., British Nuclear Energy Society, 257-271 (1974)
8. P. Kofstad and R. Bredesen, *Proc. Int. Conf. on Metallic Corrosion*, Vol 1, National Res. Council of Canada, Toronto, 12-20 (1984).
9. M. Schutz, *Oxidation of Metals*, Vol 8, 409-421 (1986).
10. V. Srinivasan and K. Vedula, *Corrosion and Particle Erosion at High Temperatures*, The Minerals, Metals and Materials Society, Warrendale, PA (1989).
11. J.H. Swisher, W.D. Cho, and S.C. Chang, in *Corrosion and Particle Erosion at High Temperatures*, The Minerals, Metals and Materials Society, Warrendale, PA, 547-564 (1989).
12. B. Chalmers, R. King, and R. Shuttleworth, *Proc. Royal Soc., A193*, 465-483 (1948).
13. P.G. Shewmon, Ohio State University, Columbus, OH, private communication.
14. J.D. Hodge, *J. Electrochem. Soc., 125*(2), 55C-57C (1978).
15. L. Himmel, R.F. Mehl, and C.E. Birchenall, *J. Metals, 5*, 827-843 (1953).
16. P.L. Surman and J.E. Castle, *Corr. Sci., 9*, 771-777 (1969).